iScience

CellPress
OPEN ACCESS

Article

TOR senses and regulates spermidine metabolism during seedling establishment and growth in maize and Arabidopsis

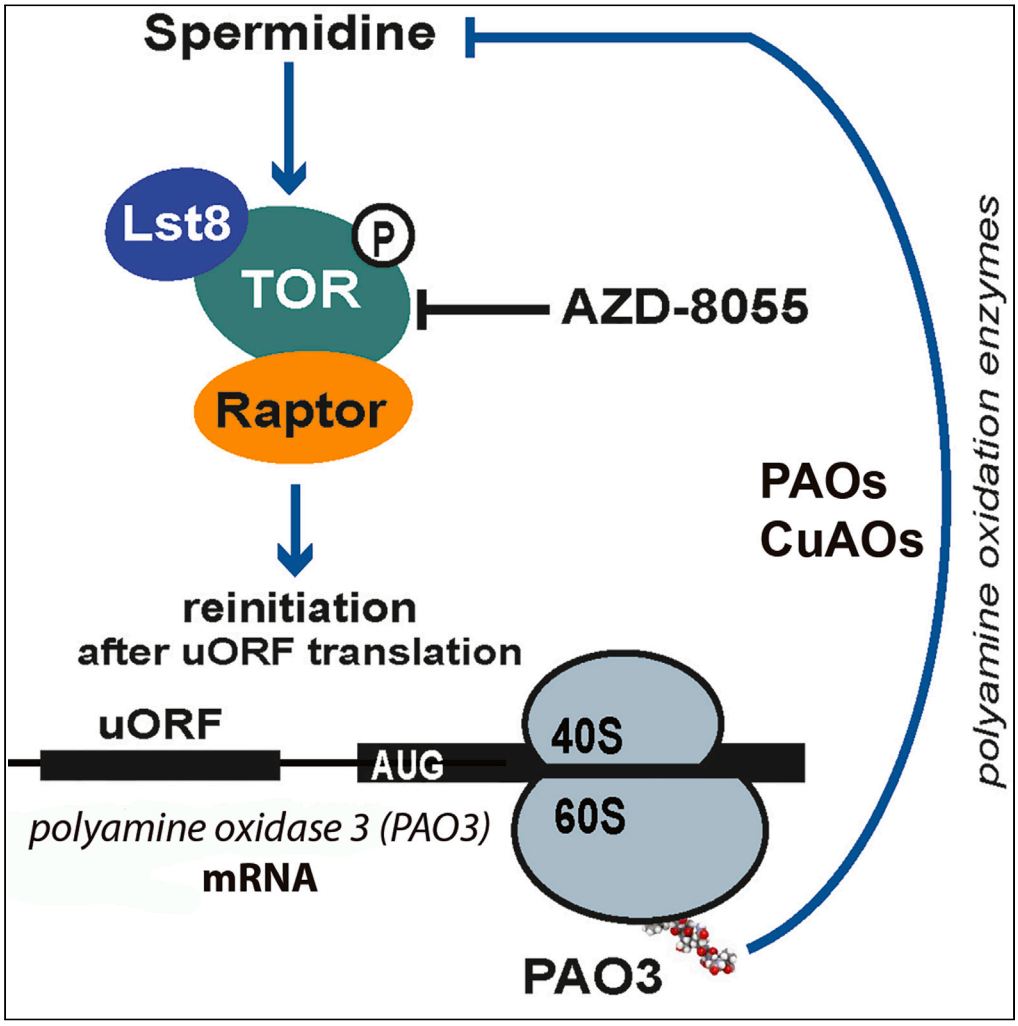

Kenia Salazar-Díaz, Yihan Dong, Csaba Papdi, Ernesto Miguel Ferruzca-Rubio, Grecia Olea-Badillo, Lyubov A. Ryabova, Tzvetanka D. Dinkova

cesy@unam.mx (T.D.D.)
lyuba.ryabova@ibmp-cnrs.unistra.fr (L.A.R.)

Highlights

Spermidine (Spd) stimulates growth of maize and Arabidopsis by activating TOR signaling

TOR stimulates translation efficiency of uORF-containing mRNAs involved in Spd catabolism

TOR provides feedback to polyamine homeostasis in response to excess of Spd

The Spd-TOR signaling axis protects maize seedlings from expeditious heat stress

Salazar-Díaz et al., iScience 24, 103260
November 19, 2021
https://doi.org/10.1016/j.isci.2021.103260

iScience

CellPress
OPEN ACCESS

Article

TOR senses and regulates spermidine metabolism during seedling establishment and growth in maize and Arabidopsis

Kenia Salazar-Díaz,[1,3] Yihan Dong,[2,3] Csaba Papdi,[2] Ernesto Miguel Ferruzca-Rubio,[1] Grecia Olea-Badillo,[1] Lyubov A. Ryabova,[2,4,*] and Tzvetanka D. Dinkova[1,*]

SUMMARY

Spermidine (Spd) is a nitrogen sink and signaling molecule that plays pivotal roles in eukaryotic cell growth and must be finetuned to meet various energy demands. In eukaryotes, target of rapamycin (TOR) is a central nutrient sensor, especially N, and a master-regulator of growth and development. Here, we discovered that Spd stimulates the growth of maize and Arabidopsis seedlings through TOR signaling. Inhibition of Spd biosynthesis led to TOR inactivation and growth defects. Furthermore, disruption of a TOR complex partner RAPTOR1B abolished seedling growth stimulation by Spd. Strikingly, TOR activated by Spd promotes translation of key metabolic enzyme upstream open reading frame (uORF)-containing mRNAs, *PAO* and *CuAO*, by facilitating translation reinitiation and providing feedback to polyamine metabolism and TOR activation. The Spd-TOR relay protected young-age seedlings of maize from expeditious stress heat shock. Our results demonstrate Spd is an upstream effector of TOR kinase in *planta* and provide its potential application for crop protection.

INTRODUCTION

Seedling establishment is a foremost phase in the plant life cycle that determines the vegetative growth and agricultural yields. Global climate change leads to unpredictable challenges at the seedling stage of crops, which impacts the further growth, development, and the final productivity. It is an important task to understand the molecular regulatory networks during seedling establishment facing expeditious stresses. Polyamines are pivotal molecules for plant development and stress adaptation in eukaryotes and have shown a great potential for crop protection (Tiburcio et al., 2014). One major type of polyamines, spermidine (Spd), is essential for embryogenesis, cell division, and protein synthesis in both plants and animals. In the monocot crop plant maize, polyamines increase in seedlings in response to salt stress, and their homeostasis is regulated by the concerted action of biosynthetic and oxidation enzymes (Jiménez-Bremont et al., 2007; Rodríguez et al., 2009). However, it remains obscure how Spd is sensed and regulates growth and stress responses.

Target of rapamycin (TOR) is a highly conserved serine/threonine protein kinase that coordinates cellular metabolism with nutrient and energy sufficiency in eukaryotes. In mammals, mTOR promotes anabolic and inhibits catabolic processes in response to growth factors, hormones, energy, and various environmental signals via two complexes, mTORC1 and mTORC2 (Liu and Sabatini, 2020). In plants, only TORC1 is conserved (Ryabova et al., 2019), and knockout mutations of the *TOR* gene in *Arabidopsis* caused embryo lethality (Menand et al., 2002). Up to now, two core subunits of TORC1, RAPTOR (regulatory associated protein of TOR) and LST8 (Lethal with Sec13 protein 8), have been described in *Arabidopsis*. Both TOR partners are encoded by two genes RAPTOR1A/RAPTOR1B and LST8-1/LST8-2, respectively (Anderson et al., 2005; Deprost et al., 2005; Moreau et al., 2012). The use of TOR-specific inhibitors and *tor RNAi* inducible mutants in *Arabidopsis* revealed its strong relevance for growth control (Deprost et al., 2007; Montané and Menand, 2013; Ren et al., 2012). TOR inactivation decreases S6K phosphorylation at the TOR-responsive hydrophobic motif residue T449 position equivalent to their animal counterparts (Schepetilnikov et al., 2011; Xiong and Sheen, 2012). The 40S ribosomal protein S6 (rpS6) was identified as major phosphorylation target of the TOR-S6K1 signaling axis among ribosomal proteins in mammals and plants (Turck et al., 2004). This

[1]Departamento de Bioquímica, Facultad de Química, Universidad Nacional Autónoma de México, Ciudad de México 04510, México

[2]Institut de biologie moléculaire des plantes, CNRS, Université de Strasbourg, 67084 Strasbourg, France

[3]These authors contributed equally

[4]Lead contact

*Correspondence: cesy@unam.mx (T.D.D.), lyuba.ryabova@ibmp-cnrs.unistra.fr (L.A.R.)

https://doi.org/10.1016/j.isci.2021.103260

pathway also operates during maize germination in response to the insulin/IGF to regulate polysomal loading of mRNAs (Dinkova et al., 2007).

Among all eukaryotes, TOR is a central nutrient sensor of nitrogen source and amino acid availability (Cao et al., 2019; Dong et al., 2017; Saxton and Sabatini, 2017). Because spermidine is a significant nitrogen sink and signaling molecule, it is intriguing to know whether TOR is affected by Spd availability. In animals, mTOR senses a precursor for Spd biosynthesis, S-adenosyl-methionine (SAM), through SAMTOR (Gu et al., 2017). Interestingly, to form Spd, SAM is catalyzed by decarboxylase SAMDC/AMD1 whose stability is also controlled by mTOR (Zabala-Letona et al., 2017).

In plants, polyamine metabolism is largely controlled by the metabolic genes that harbor upstream open reading frames (uORFs) within their leader regions (von Arnim et al., 2014). uORFs located within the leaders of up to 40% of total mRNAs in *Arabidopsis* are considered as prevalent translation repressors that are under the control of TOR (Schepetilnikov et al., 2013). When TOR is activated by auxin, the ROP2-TOR-S6K1 signaling axis promotes phosphorylation of eukaryotic translation initiation factor 3 subunit h (eIF3h) and thus translation reinitiation of uORF-containing mRNAs (Schepetilnikov et al., 2013, 2017).

Up to now, the relationship between the TOR signaling pathway and polyamines remains unexplored in *planta*. Here we used the monocot crop plant maize and the model organism *Arabidopsis thaliana* to show an important role of Spd-TOR relay in early seedling establishment. We discovered that Spd activates TOR and active TOR facilitates production of polyamine metabolic enzymes through translation reinitiation. According to this, Spd acts as an upstream effector of TOR and provides a feedback-regulation of Spd metabolism by TOR during early seedling growth. We suggest that Spd employs TOR signaling for protection of crop seedlings from heat stress.

RESULTS

Spermidine impacts growth in maize through active TOR that accumulates during earlier stages of seedling establishment

Polyamines are nitrogenous signaling molecules, which can impact on germination and growth and thus may collaborate with TOR that is a central nutrient sensor. Here, we aimed to test whether polyamines can mediate their effect on growth through the TOR signaling pathway. We selected Spd, one of the most abundant polyamines in plants, which, in contrast to spermine (Imai et al., 2004a), is essential for survival in *Arabidopsis* (Imai et al., 2004b).

To determine first how TOR is activated during earlier seedling stages in maize, we tested the ZmTOR activation status using phospho-specific antibodies, anti-(mTOR-S2448-P), as well as the downstream target S6K1 phosphorylation status at the *At*TOR specific hydrophobic motif residue T449 and phosphorylation of rpS6 at the S6K1-dependent residue Ser240 (S240) in maize seeds before and after 24 h or 48 h of imbibition (Figure 1A). mTOR S2448 appears to be conserved in maize and *Arabidopsis* TOR and corresponds to S2424 in *Arabidopsis* TOR (Agredano-Moreno et al., 2007; Schepetilnikov et al., 2013). Except in dry seeds, we observed phosphorylation of TOR at 24 h of seed imbibition, which was further increased at 48 h (Figure 1A). Both S6K1 and RPS6 were found in dry seeds, but no detectable phosphorylation was found at the tested residues. However, S6K1 and RPS6 were found phosphorylated in extracts prepared from isolated axes and roots, after 24-h imbibed conditions, confirming the active status of TOR after 24 h of seed imbibition (Figure 1A). Although, we detected *TOR*, *Lst8*, *Raptor*, *S6K1*, and *RPS6* transcripts (Woodhouse et al., 2021) in maize seeds, only the *TOR*, *S6K1*, and *RPS6* transcript levels were further increased during seed imbibition (Figure S1 and Table S1). Albeit S2448 phosphorylation has been used to measure TOR activation in plants, recent reports exposed limitations on its use in mammals (Casagrande Figueiredo et al., 2017). Thus, measurements of TOR phosphorylation using anti-(mTOR-S2448-P) were excluded from further analysis, and we employed S6K1 and RPS6 phosphorylation as valuable readouts for activation of the TOR pathway. We next tested whether TOR inactivation impairs maize seedling growth specifically. The embryonic axes preimbibed for 45 h were treated with a second-generation TOR inhibitor AZD-8055 (Montané and Menand, 2013; Schepetilnikov et al., 2017) for 3 h (Figure 1B). The level of TOR activity observed at 48 h was reduced by AZD-8055 in a dose-dependent manner as manifested by the decrease in downstream S6K1 and RPS6 phosphorylation levels (Figure 1B). To demonstrate that TOR is required for growth during the earlier stage of seedling establishment, we dissected embryonic axes from maize germinated seeds and performed a 3-d treatment with different AZD-8055 concentrations.

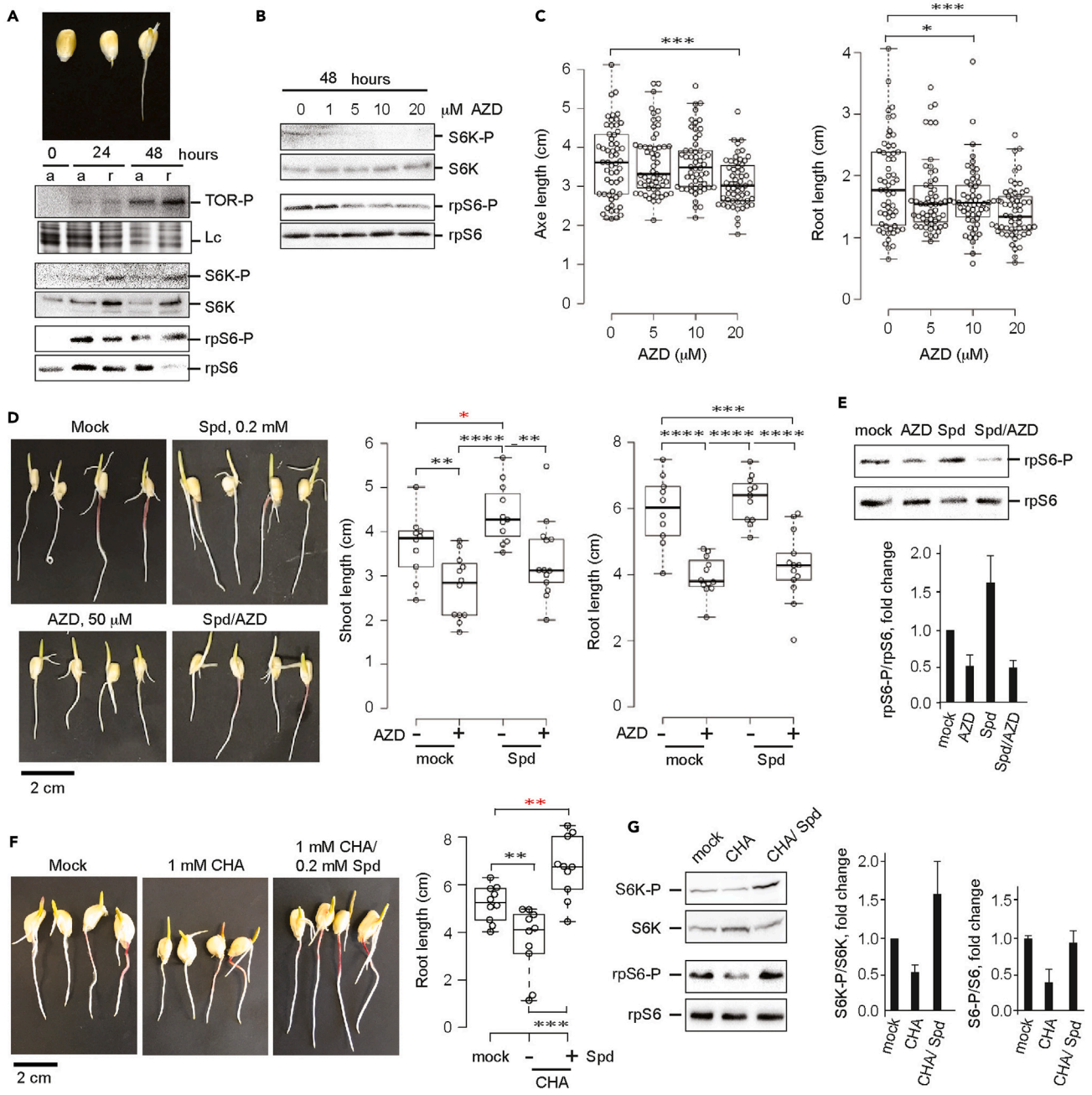

Figure 1. Exogenous Spd promotes seedling growth in AZD-8055- and CHA-sensitive manner

(A) Representative images of Chalqueño maize seed germination and seedling growth at 24 h and 48 h of imbibition. *Bottom* Immunoblot analysis of phosphorylated TOR (TOR-P); S6K-P/S6K and rpS6-P/rpS6 in whole axes and root tissues. Lc: loading control by Coomassie staining.

(B) Immunoblot analysis of phosphorylated S6K-P/S6K and rpS6-P/rpS6 in whole embryonic axes without (DMSO, solvent) or with AZD-8055 added to dissected axes at 45 h of seed imbibition as indicated.

(C) Quantification of whole embryonic axes and root lengths after 3 days of treatment with different AZD-8055 concentrations as indicated (n = 20).

(D) 24-h imbibed maize seeds were further incubated in water (mock) or 0.2 mM Spd with (+) or (–) without 50 μM AZD-8055 (AZD) at 28°C for 48 h (n = 10). Scale bar refers to seedling length.

(E) Immunoblot analysis of rpS6 total and phosphorylated at S240 (rpS6-P) levels in root tips. (*Bottom panel*) Specific rpS6 phosphorylation was estimated as rpS6-P/rpS6 ratio from four independent experiments. Representative immunoblot is shown (n = 4).

(F) 24-h imbibed maize seeds were incubated in water (mock), 1 mM CHA, or 1 mM CHA with 0.2 mM Spd (n = 10) during 48 h. Scale bar refers to seedling length.

Figure 1. *Continued*

(G) Immunoblot analysis of total S6K1 and rpS6 levels and the levels of S6K1 phosphorylated at T449 (S6K1-P) and rpS6 phosphorylated at S240 (rpS6-P) in embryonic axes isolated from 24-h imbibed seeds treated with 1 mM CHA or 1 mM CHA with 0.2 mM Spd at 28°C during 24 h. (*Right panel*) Specific S6K or rpS6 phosphorylations were estimated as S6K-P-T449/S6K or rpS6-P-S240/rpS6 ratios from three independent experiments. Representative immunoblot is shown (n = 3) for each case.

Data information: values were presented as boxplot with median ±s.d. (C, D, and F) and bar chart with mean ± s.d. (F). Statistical test was performed by one-way ANOVA followed by two-tailed t test: $p < 0.05$ *, $p < 0.01$ **, $p < 0.001$ ***, $p < 0.0001$****.

Our results showed that TOR inactivation led to a significant decrease in embryonic axe length at 20 μM AZD8055, whereas the root elongation was significantly affected even at 10 μM AZD-8055 (Figure 1C).

To test the relationship between TOR and Spd pathways, we first added the polyamine Spd to nongerminated seeds (Figure S2), as Spd was shown to activate germination rate (Huang et al., 2017). We observed a tendency to greater root length at 48 h, although there was a high sample variability during germination (Figures S2A and S2B). However, Spd-treated seedling growth was highly sensitive to AZD-8055 (50 μM), indicating that TOR active status is important for Spd-treated maize. Higher AZD-8055 concentration was applied to whole seeds as compared with dissected embryonic axes (see STAR Methods). A longer incubation period for Spd-treated seedlings led to a significant effect of Spd on root growth (Figure S2B, right panel). Strikingly, the enhanced growth of Spd-treated seedlings was fully abolished by AZD-8055 reaching the level corresponding to mock seedlings. Spd application resulted in an increase of S6K phosphorylation, which was nearly abolished upon both Spd and AZD-8055 application (Figure S2C).

To further verify our hypothesis, we modified our experimental set up and used the 24 h postgerminated seeds to perform 0.2 mM Spd treatment in the absence or the presence of 50 μM AZD-8055 for the next 48 h of seedling growth. The results showed that Spd soaking significantly increased shoot length of postgerminated seeds at 48 h of treatment, whereas there was practically no difference in root length between the mock- and Spd-treated seedlings (Figure 1D). Strikingly, AZD-8055 application impaired growth of both mock- and Spd-treated seedlings. We also analyzed the phosphorylation of rpS6 at S6K1-dependent Ser240 (S240) to compare TOR responses with AZD-8055 treatment (Dobrenel et al., 2016). Given that Spd treatment increased rpS6 phosphorylation at S6K1-sensitive S240 in AZD-8055-dependent manner (Figure 1E), we concluded that this polyamine positive effect on postgerminated seedling growth might depend on ZmTOR pathway activation. These data further strengthen our hypothesis that polyamine signaling requires TOR activity to impact on the early postgermination seedling growth.

To further test the specificity of Spd on TOR activation and root elongation, we used the cyclohexylamine (CHA) to inhibit Spd synthesis in the 24-h postgerminated seeds during 48 h. As expected, 1 mM CHA was sufficient to significantly reduce root length (Figure 1F) and resulted in a significant decrease in both S6K and rpS6 phosphorylation (Figure 1G). Strikingly, seedlings pretreated with 1 mM CHA and 0.2 mM Spd during 48 h nearly restored the Spd effect on root growth. As expected, application of Spd with CHA was sufficient to restore S6K and rpS6 phosphorylation (Figure 1G). Thus, we concluded that Spd can induce TOR activation and earlier seedling growth in AZD-8055- and CHA-sensitive manner.

Spermidine can activate TOR signaling in *Arabidopsis*

To gain more genetic insight into the Spd-TOR relay, we next investigated the effect of exogenous Spd on TOR activation and seedling growth in *Arabidopsis*. Importantly, Spd significantly increased *Arabidopsis* seedling growth at 0.01 mM concentration and further promoted root elongation at 0.1 mM concentration (Figure 2A). In addition, TOR inactivation by AZD-8055 caused a decrease in root elongation of Spd-treated seedlings, but at lesser extend as compared with that in mock seedlings, likely due to higher levels of active TOR in Spd-treated seedlings. We also performed immunoblot analysis of TOR-dependent phosphorylation of S6K1 at conserved TOR-specific hydrophobic motif residue T449 under different exogenous Spd concentrations. S6K is a TOR downstream target and its canonical signaling output marker in mammals and plants (Schepetilnikov et al., 2011; Xiong and Sheen, 2012). As expected, the level of S6K1 phosphorylation at T449 in Spd-treated seedlings was increased as compared with mock seedlings about 1.3- and 1.7-fold by 0.01 and 0.1 mM Spd, respectively, whereas decreased by AZD-8055 treatment in all tested conditions (Figure 2B). It is worth noting that growth arrest caused by TOR inactivation in the 0.1-mM Spd-containing media was less pronounced and S6K1 phosphorylation levels remained more than 2-fold higher than in the case of using inhibitor alone (Figure 2B). This suggests that 0.1-mM Spd-treated seedlings

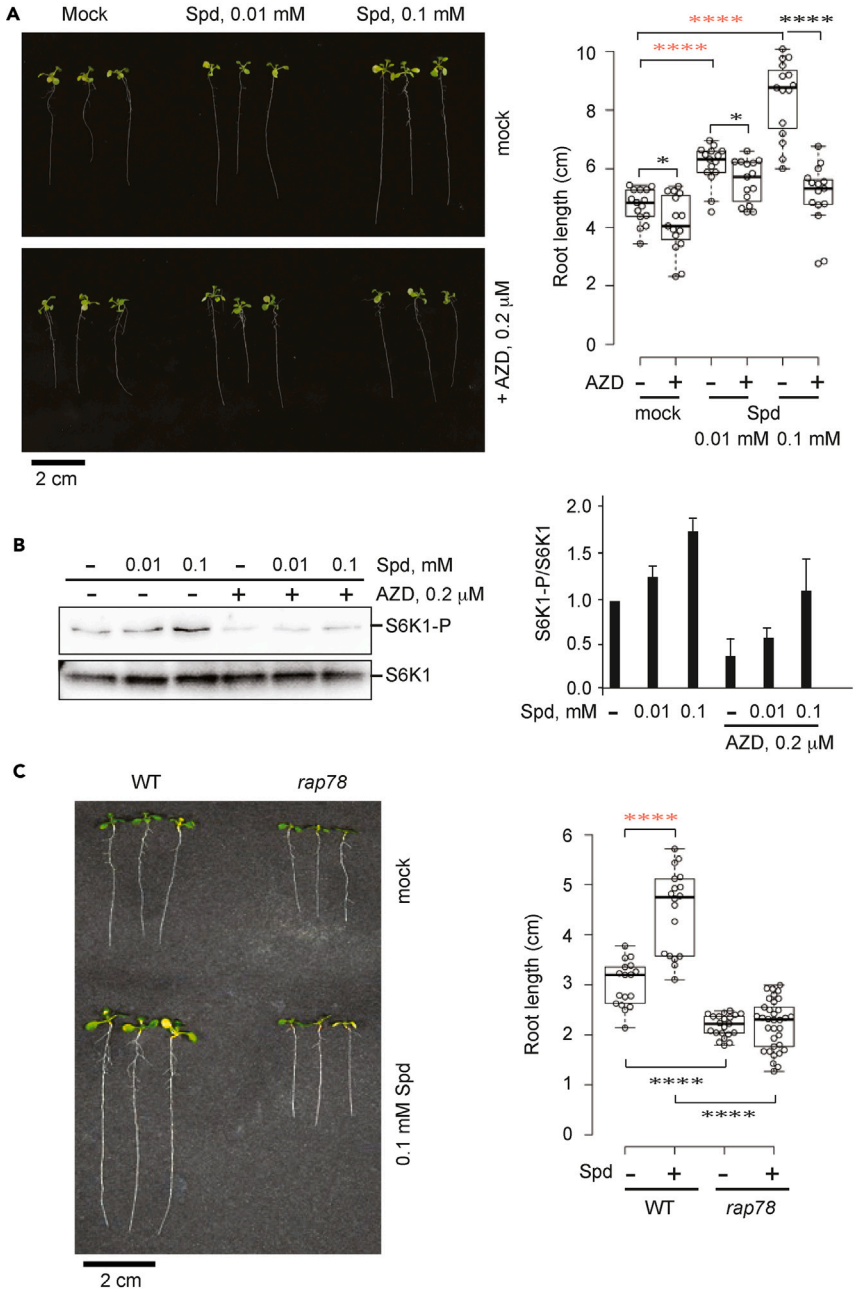

Figure 2. Exogenous Spd boosts seedling growth in Arabidopsis through the TORC1 pathway

(A) Arabidopsis seedlings were grown for 14 days on 1/2 Murashige and Skoog (MS) medium plus 0.5% sucrose (mock), supplemented with 0.01 or 0.1 mM Spd without (–) or with 0.2 μM AZD-8055 at 22°C under long photoperiod for two weeks. Representative images of whole plantlets and quantification of root length are shown (n = 15). Scale bar refers to root length.

(B) Immunoblot analysis of total S6K1 levels and the levels of S6K1 phosphorylated at T449 (S6K1-P) in 14-days-old seedlings. (*Right panel*) Specific S6K phosphorylation was estimated as S6K-P-T449/S6K ratio from three independent experiments.

(C) Col-0 and *rap78* were grown for 14 days on 1/2 MS medium plus 0.5% sucrose (mock), supplemented with 0.1 mM Spd at 22°C under long photoperiod for two weeks (n = 15). Scale bar refers to root length.

Data information: values were presented as boxplot with median ±s.d. (A, C). Statistical test was performed by one-way ANOVA followed by two-tailed t test: $p < 0.05$ *, $p < 0.01$ **, $p < 0.001$ ***, $p < 0.0001$****.

showing higher levels of active TOR are less sensitive to AZD-8055 inhibition and supports Spd as an upstream effector of TOR in promoting plant growth.

The fact that Spd promotes phosphorylation of S6K1 in AZD-8055-sensitive manner suggests that Spd acts through the TORC1 complex for its downstream effects. Given that Raptor is required to recruit substrates of TORC1 for their phosphorylation by TOR, we tested whether *RAPTOR1B knockout line rap78* (Kravchenko et al., 2015) would support increased growth in response to Spd. *rap78* mutants have their root growth decreased as expected (Figure 2C, left panel). Although WT *Arabidopsis* seedlings have their growth accelerated by 2-fold when grown on medium containing 0.1 mM Spd, *rap78* mutant plants lost their capacity to respond to Spd, indicating that Spd signals through the TORC1 complex. These data strongly suggest that Spd functions upstream of TOR and requires RAPTOR1B to activate TOR-S6K1 signaling relay and thus seedling growth.

TOR activates translation reinitiation of uORF-containing *CuAO1* and *PAO3* mRNAs

In eukaryotes polyamine levels are regulated through many metabolic enzymes encoded by mRNAs that harbor uORFs within their leader regions. For example, S-adenosyl methionine decarboxylases (SAMDCs) required for polyamine biosynthesis, copper-dependent amine oxidases (CuAOs), and FAD-dependent polyamine oxidases (PAOs) that catalyze terminal oxidation and back conversion of polyamines, respectively, are encoded by uORF-containing mRNAs (Figure S3 and Tables S2–S3). It was shown that TOR, when activated by the phytohormone auxin, overcomes the inhibitory pressure of uORFs and promotes translation of uORF-containing mRNAs (Schepetilnikov et al., 2013, 2017).

To shed light on the role of TOR in translation reinitiation in maize, we compared polysomal association of uORF-containing endogenous mRNAs such as *PAO3* and *SAMDC* in extracts prepared from the 48-h dissected embryonic axes, treated or not with 20 μM AZD-8055 for 3 h, by employing sucrose density gradients (Figure 3A). Comparative polysome profile analysis in wild-type (WT) and AZD-8055-treated seedling-derived extracts suggested that 20 μM AZD-8055 treatment partially reduced the polysome/monosome ratio in WT extracts by about 20% (Figure 3A, left panel). *PAO3* mRNA, preferentially detected only in light polysomes of mock plants, was shifted to the fraction of monosomes in response to AZD-8055 treatment, again uncovering translation suppression by the TOR inhibitor (Figure 3A, right panel). The results showed a shift in *SAMDC* mRNA from heavy to the medium polysomal fractions, suggesting inhibition of translation by uORFs upon TOR inactivation. It should be noted that *SAMDC* 5′UTRs contain the so-called conserved peptide uORF (CPuORF; (Shantz et al., 1994; Franceschetti et al., 2001); see Figure S3), which encodes a peptide causing ribosome stalling at the stop codon of CP uORF in the presence of high Spd levels in mammals and plants (Hanfrey et al., 2005; Hill and Morris, 1992; Ryabova and Hohn, 2000). However, under normal level of polyamines, the CPuORF2 is often bypassed by ribosomes that translate uORF1. In contrast, distribution along the sucrose gradient of uORF-less mRNAs—*rpS6* and *eIF4E* (*eukaryotic translation initiation factor 4E*)—was either not affected or slightly increased in LP by AZD-8055. No changes in mRNA abundances were observed for any of the analyzed transcripts under 20 μM AZD-8055 application (Figure 3B).

To further validate that the Spd-TOR relay regulates growth via promoting synthesis of proteins from uORF-mRNAs, we tested whether TOR activation by Spd or auxin impacts translation reinitiation in *Arabidopsis* mesophyll protoplasts. In a first experimental set up, protoplasts derived from WT or TOR-deficient 35-7 RNAi plants (Deprost et al., 2007) were transfected with reporter gene harboring a single beta-glucuronidase (*GUS*) construct placed downstream of a short unstructured leader (p*monoGUS*) or *AtCuAO1* 5′UTR (p*AtCuAO1-GUS*) and p*monoGFP*, containing a single *GFP* ORF (control for transformation efficiency; Figure 3C). As expected, reinitiation of *AtCuAO1-GUS* was about 40% less efficient in TOR-deficient as compared with WT protoplasts, whereas *monoGUS* expression in 35-7 protoplasts was only 20% less efficient than in WT (Figure 3D).

Next we tested the effect of Spd and auxin on p*ZmPAO3-GUS* and p*AtCuAO1-GUS* expression in the absence or presence of AZD-8055 using the same experimental set up. In these experiments, we did not include maize *SAMDC* 5′ UTR to avoid any repression of GUS ORF translation by the product of CPuORF2 at increased Spd levels. In contrast to the p*monoGUS* uORF-less leader, the *ZmPAO3* leader fused to the *GUS* ORF in its authentic initiation context (p*ZmPAO3-GUS*) reduced *GUS* ORF translation by about 7-fold and *AtCuAO1* leader by about 14-fold, suggesting that uORFs become nearly reinitiation nonpermissive in

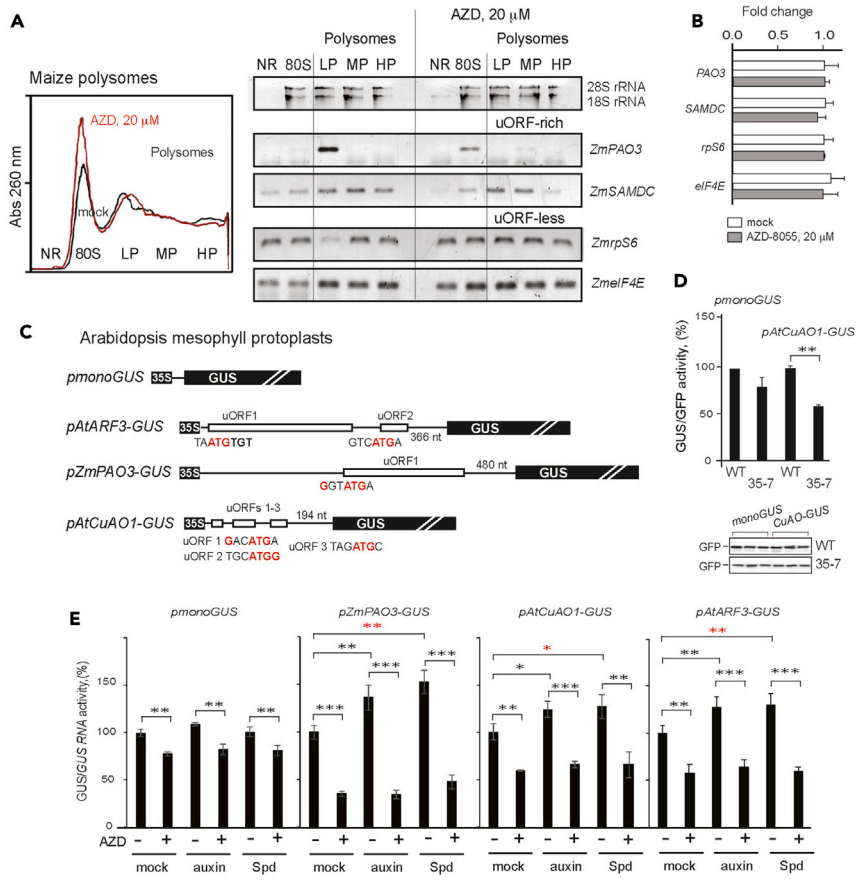

Figure 3. *PAO* and *CuAO* translation reinitiation is activated in response to both Spd and TOR in AZD-8055-sensitive manner

(A) Polysomes from 48-h imbibed embryonic axes not treated (black line) or treated (red line) with 20 μM AZD-8055 were subjected to velocity sedimentation through sucrose density gradient. Gradients were fractionated while scanning at 260 nm, and the resulting absorbance profiles are shown. Fractions were collected and pooled as NR (no ribosome), 80S (monosomes), LP (light polysomes), MP (medium polysomes), and HP (heavy polysomes), and RNA was analyzed by RT-qPCR for transcripts indicated on the right of each gel along the profile (n = 2). Positions of 18S and 28S rRNA are shown.

(B) *ZmSAMDC*, *ZmPAO3*, *ZmrpS6*, and *ZmeIF4E* transcript abundances were evaluated by RT-qPCR in 48-h imbibed embryonic axes treated or not treated with 20 μM AZD-8055 (n = 2). *Actin* was used as the normalization control and results expressed as fold change relative to mock.

(C) Schematic representation of constructs containing the GUS reporter with either short or uORF-containing 5′UTR used for transformation of mesophyll protoplasts.

(D) Transfection experiments in Arabidopsis WT or 35-7 RNAi mesophyll protoplasts included one reporter plasmid as indicated and transfection control plasmid p*mono*GFP. The GUS/GFP in mock protoplasts was set as 100% for p*monoGUS* (250,000 relative fluorescence units, RFU). GFP levels were estimated by western blot (*bottom panel*).

(E) WT mesophyll protoplasts were transfected with reporter plasmids shown in (C) as indicated. After transfection, cells were incubated or not incubated (mock) with 1 μM NAA or 0.1 mM Spd in the presence or not of 0.5 μM AZD-8055 for 18 h (n = 3). mRNA integrity and levels were estimated by semiquantitative RT-PCR. GUS/*GUS RNA* ratios were calculated and shown as black bars. The GUS/*GUS RNA* in mock protoplasts was set as 100% for p*monoGUS* (200,000 relative fluorescence units, RFU); p*ZmPAO3-GUS* (30,000 RFU); p*CuAO1-GUS* (20,000 RFU); and p*ARF3-GUS* (50,000 RFU).

Data information: values were presented as bar chart with mean ± s.d. (B and C). Statistical test was performed by one-way ANOVA followed by two-tailed t test: $p < 0.05$ *, $p < 0.01$ **, $p < 0.001$ ***, $p < 0.0001$****.

mock conditions. This low level of p*ZmPAO3-GUS* expression was significantly increased by auxin and further enhanced by Spd. Importantly, the protoplast response to both auxin and Spd was abolished by AZD-8055 (Figure 3E). Three short uORFs of *AtCuAO1* leader were less responsive to either auxin or Spd, but their positive effects were abolished by AZD-8055. We noted that AZD-8055 was efficient in suppressing uORF-containing mRNA expression by at least 50% in mock protoplasts while p*mono*GUS

expression decreased to a lesser extent. The levels of *GUS*-containing RNAs were unaltered during protoplast incubations (data not shown). Next we assayed whether the Spd-TOR signaling axis has a general role in promoting translation reinitiation of uORF-mRNAs that do not encode polyamine-biogenesis-related proteins. As expected, both auxin and Spd can increase translation of *auxin response factor 3* (*ARF3*) mRNA in AZD-8055-senstitive manner (Figure 3E), indicating that TOR activated by either auxin or Spd has a general effect on reinitiation after uORF translation (Schepetilnikov et al., 2013).

Our results show that Spd activates translation of *CuAO1* and *PAO3* acting through TOR. Thus, the Spd-TOR relay can impact production of polyamine-biosynthesis-related enzymes, if these are encoded by uORF-containing mRNAs. The data presented above indicate that TOR governs production of SAMDC and polyamine oxidases in an AZD-sensitive manner. Hence, uORF control is required to balance and maintain proper polyamine levels for growth and stress responses.

The Spd-TOR signaling axis attenuates heat stress susceptibility of maize

Polyamines and especially Spd have been implicated in protecting rice and wheat seedlings from heat-induced damage (Jing et al., 2020; Mostofa et al., 2014; Tang et al., 2018). However, how Spd can alleviate the consequences of high temperature remain to be investigated. Given increasing climate-induced yield losses for many crops each year, we attempted to further investigate a capacity of the Spd-TOR signaling relay to alleviate the heat injury of maize seedlings at earlier stages of their establishment and growth.

To evaluate TOR dependency, maize seeds imbibed for 24 h were soaked without or with 0.2-mM Spd either in the absence or in the presence of AZD-8055 for 48 h at ambient temperature 28°C. Then plantlets were either further maintained at 28°C or transferred to 42°C for additional 72 h (Figure 4). Although treatment with 0.2 mM Spd of seedlings growing for 6 days at normal temperature did not show great impact on growth (Figure 4A), shoot and root length were highly sensitive to AZD-8055 and decreased significantly, indicating active TOR state at 28°C. Plantlets grown under heat stress showed significant damage and strong delay in development as compared with seedlings grown at normal temperature (Figure 4B). In contrast, Spd treatment positively affected growth by significantly improving root and shoot elongation (Figure 4B, Spd). Strikingly, the protective effect of Spd was abolished in the presence of AZD-8055, confirming that the connection between polyamines and TOR operates under stress conditions.

DISCUSSION

Until now it was unclear how polyamine levels are sensed and participate in seed germination and growth. However, genetic evidence suggests that spermidine, but not spermine (Imai et al., 2004a), plays an essential role in plant embryo development, given that disruption of both genes encoding spermidine synthase lead to embryo lethal phenotype at the heart-torpedo transition stage in *Arabidopsis* (Imai et al., 2004b). Interestingly, double-mutant seeds are deficient in Spd, whereas they accumulate high levels of its precursor, putrescine. Here we discover that Spd promotes seedling growth through the TORC1 signaling pathway in *Arabidopsis* and maize.

We have demonstrated an increase in the level of active TOR during maize seed germination and postgerminative growth. Inactivation of TOR decreases the embryonic axes and roots growth due to insufficient TOR signaling and S6K activity. Our study uncovered the involvement of the TOR signaling pathway in perception and transduction of the Spd signal toward balancing cellular homeostasis and sustained growth in *Arabidopsis* dicot and maize crop plants. First, Spd promotes growth in TOR inhibitor AZD-8055-sensitive manner in maize and *Arabidopsis*. Further, TOR was activated in the presence of Spd and assists seedling growth, whereas either genetic or pharmaceutical inhibition of TOR slowed down growth and abolished growth stimulation by Spd. In contrast, cyclohexylamine (CHA) that inhibits Spd biosynthesis abolished the phosphorylation of S6K and, accordingly, reduced root elongation during maize seedling development. When CHA and Spd were applied together we observed a strong recovery of the CHA-mediated seedling growth defect. These results demonstrate that TOR pathway activation by Spd leads to enhanced root elongation and seedling growth.

TORC1 ability to phosphorylate target substrates depends on the activity of a conserved eukaryotic TOR-binding partner, RAPTOR, which presents substrates to TOR for phosphorylation (Schalm and Blenis, 2002; Liko and Hall, 2015). RAPTOR binding to the TOR HEAT (Huntington, EF3A, ATM, TOR) domain was demonstrated in both *Arabidopsis* and the green alga *Chlamydomonas reinhardtii* (Anderson et al.,

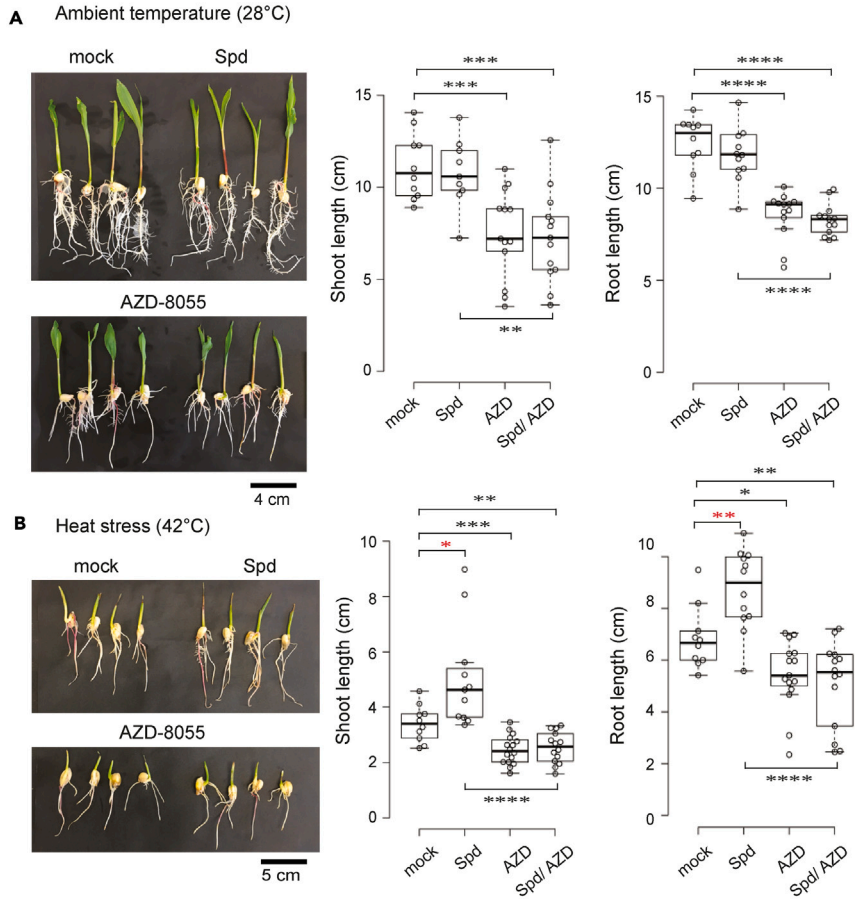

Figure 4. Spd-TOR signaling alleviates heat stress damage in maize seedlings

(A and B) Representative images of 6-day-old maize seedlings grown at 28°C (A) or 42°C (B) under long photoperiod in water (mock) or supplemented with 0.2 mM spermidine (Spd) in the presence (+) or not (–) of 50 μM AZD-8055 (n = 15). Scale bars refer to seedling length.

Data information: values were presented as boxplot with median ±s.d. (A and B). Statistical test was performed by one-way ANOVA followed by two-tailed t test: $p < 0.05$ *, $p < 0.01$ **, $p < 0.001$ ***, $p < 0.0001$****.

2005; Deprost et al., 2007; Mahfouz et al., 2006; Moreau et al., 2012), suggesting conserved mechanism of RAPTOR function in TORC1. Our genetic experiments demonstrated that the induction of growth by Spd was downregulated in the *rap78 Raptor 1b* knockout mutant, suggesting that Raptor can mediate Spd-activated TOR action *in planta*. Given that the Spd-promoted TOR signaling activity is reduced by AZD-8055 application to the mock plant and decreased in conditions of RAPTOR deficiency, we conclude that Spd and TOR signaling acts in a common pathway to control plant growth. In plants, the number of upstream effectors of TOR signaling is growing—phytohormone auxin, growth factors, nutrients, and light (Garrocho-Villegas et al., 2013; Schepetilnikov et al., 2013; Xiong et al., 2013; Li et al., 2017; Schepetilnikov and Ryabova, 2017; Shi et al., 2018). Our study provides evidence that Spd is a strong candidate to function as upstream effector of TOR. According to our data, Spd triggers phosphorylation of S6K1 at TOR-specific hydrophobic motif residue T449, and ribosomal protein S6 at S240, indicating the canonical TOR signaling pathway is likely to be involved in the perception of the Spd signal.

Our data suggested that TOR not only sensed Spd availability but also finetuned Spd homeostasis through a posttranscriptional mechanism. Indeed, previous work in *Arabidopsis* demonstrated that AtTOR positively modulates total mRNA translation (Deprost et al., 2007). In eukaryotes, mRNAs in polyamine catabolism (*PAOs* and *CuAOs*) are enriched by inhibitory uORFs that impede their translation (von Arnim et al., 2014; Guerrero-González et al., 2014; Schepetilnikov and Ryabova, 2017). In *Arabidopsis*, inefficient translation of uORF mRNAs could be attenuated by the auxin-ROP2-TOR signaling axis

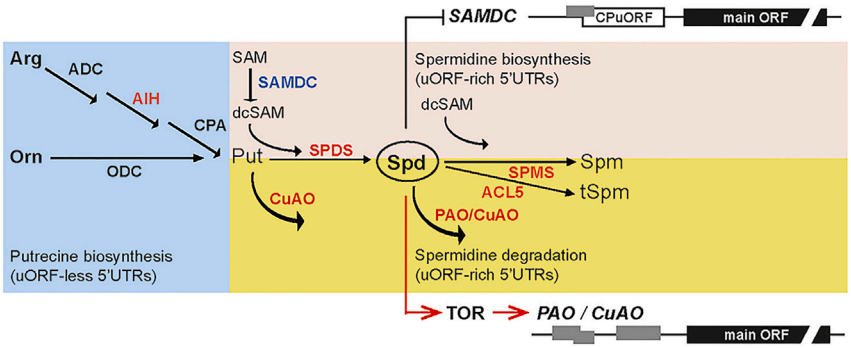

Figure 5. uORF allocation among the polyamine metabolic network: effects of TOR and/or Spd on polyamine synthesis and degradation

(*Blue box*) Putrescine biosynthesis pathways from arginine or ornithine are presented by arginine decarboxylase (ADC), agmatine iminohydrolase (AIH), N-carbamoylputrescine amidohydrolase (CPA), and ornithine decarboxylase (ODC)—encoded largely by uORF-less mRNAs.

(*Pink box*) S-adenosyl-methionine (SAM), if decarboxylated by S-adenosylmethionine decarboxylase (SAMDC), is used for Spd synthesis. *SAMDC* mRNA 5′UTR contains conserved peptide (CP) uORF.

(*Yellow box*) Spd degradation pathways are presented by FAD-dependent polyamine oxidases (PAOs), spermine synthase (SPMS), and thermospermine synthase (ACL5) encoded by uORF-rich mRNAs.

(*Top right*) High Spd can arrest SAMDC synthesis via CP uORF.

(*Bottom right*) The Spd-TOR signaling axis can positively regulate translation competency of PAOs and copper-dependent amine oxidases (CuAOs).

(Schepetilnikov et al., 2013, 2017). We have shown that TOR inactivation by AZD-8055 causes defects in polysomal loading of endogenous maize uORF-containing *PAO3* (Figure 3A), strongly suggesting that TOR inhibition contributes to decreased uORF-mRNA translation in maize. AZD-8055 treatment interferes with CP uORF-*SAMDC* association with only heavy polysomes in our conditions (Figure 3A). The results in plant mesophyll protoplasts confirmed the role of Spd in translation of *PAO3*, *CuAO1* and unrelated to polyamine metabolism *ARF3* in AZD-8055-sensitive manner (Figure 3E), suggesting that TOR, if activated by either auxin (Schepetilnikov et al., 2013) or Spd, promotes translation initiation of uORF-containing mRNAs. Indeed, we observed a strong defect in *CuAO1* 5′UTR-mRNA translation in TOR-deficient plants and an increase in both *CuAO1* and *PAO3* leader-driven expression in protoplasts treated with auxin or Spd. In both cases, inactivation of TOR nearly abolished uORF-mRNA translation in mock-, auxin-, or Spd-treated protoplasts. Thus, Spd can promote translation of polyamine degradation enzymes through the TOR pathway.

Our data reveal a simple view of the mRNA-specific features such as inhibitory 5′UTR uORFs and mechanisms that confer Spd-TOR-dependent translation control in Spd biogenesis. The subset of uORF-mRNAs that are specifically regulated by TOR consists almost entirely of transcripts for polyamine oxidases, PAOs and CuAOs, in addition to spermidine synthase (SPDS), spermine synthase (SPMS), and thermospermine synthase (ACL5) (Guerrero-González et al., 2014; Moschou et al., 2012; von Arnim et al., 2014) (see Figure 5, yellow panel; Figure S3 and Tables S2–S3). We find no uORF-rich transcripts for synthesis of putrescine from either arginine or ornithine, except of *agmatine iminohydrolase* (*AIH*) mRNA that can harbor several uORFs (Figure 5, blue panel; Table S3). Spd synthesis depends on decarboxylation of SAM by SAMDC (Figure 5, pink panel). *SAMDC* mRNA is among the PA-responsive transcripts with a short uORF preceding the CPuORF (Franceschetti et al., 2001); high PA concentrations lead to CP uORF translation that results in SAMDC synthesis suppression (Hanfrey et al., 2005; Figure 5, top right).

Here we propose a model, which states that Spd-TOR signaling differentially controls the Spd homeostasis by regulating translation competence of uORF-containing mRNAs. We found that Spd-related catabolic enzymes such as polyamine oxidases are the main targets of uORFs responsible for maintaining the moderate Spd levels. Indeed, TOR inactivation by AZD-8055 strongly correlated with translational repression of *PAO5′UTR*- or *CuAO 5′UTR*-driven reporter (Figure 3E). This is likely the consequence of a negative feedback in response to the excess of Spd. Moreover, high Spd will trigger CP-uORF translation, to arrest SAMDC synthesis and function of spermidine and spermine synthases (Hanfrey et al., 2005). Recent work by Guerrero-González et al. (2014) suggested that although 168 nt *AtPAO2* uORF inhibits downstream

main ORF translation, increase in exogenous polyamine levels promotes downstream reporter expression with both native *AtPAO2* and *35S* promoter, thus alleviating the negative effect of *AtPAO2* uORF. The Spd positive effect on *AtPAO2* mRNA translation is consistent with our model, where TOR activated by Spd can increase reinitiation of *ZmPAO3* after translation of upstream uORF.

In addition, analysis of currently available transcriptomic data (Caldana et al., 2013; Xiong et al., 2013; Dong et al., 2015) revealed no significant differences in the levels of mRNAs that encode enzymes involved in Spd biogenesis upon application of TOR inhibitors (see Table S3). These results argue that translation of uORF-containing mRNAs is highly sensitive to TOR activation and that this is the basis of their regulation by Spd. However, we cannot rule out mRNA isoforms that appear as a result of alternative splicing events, which can change the position and/or number of uORFs.

Our observation of active TOR requirement for facilitating production of PAOs and CuAOs that catalyze PA oxidation is consistent with previously published data demonstrating a shift into putrescine at the expense of spermidine in TOR inactivation conditions (Caldana et al., 2013) and with a 5′UTR dependence of *Arabidopsis SAMDC* expression in root meristems at early germination stages (Majumdar et al., 2017). Thus, the concerted action of uORF regulatory mechanisms under the control of Spd and TOR can balance spermidine homeostasis to regulate growth in response to various environmental conditions.

Spd, when applied exogenously, is involved in protecting crops from stress-induced damage (Chen et al., 2019; Huang et al., 2017; Rodríguez et al., 2009). The observations of requirements for high levels of free Spd and Spm in salt stress conditions (Duan et al., 2008) are consistent with a central role of Spd-TOR relay in increasing tolerance of maize seedlings to heat stress damage (Figure 4B). Indeed, our results indicate that the Spd-TOR signaling axis helps young-age seedlings of maize to alleviate heat stress damage to a certain extent.

In conclusion, our results suggest that Spd can link TOR regulation of translation with plant adaptation to environmental and internal cues. Molecular actors in such regulation, as well as the impact of Spd on TOR activity on the proteome and metabolic profiles, are awaiting future investigation to bring a better understanding of plant physiology and breeding proposals. The knowledge gain on regulatory mechanisms that impact gene expression at these stages would be of utmost relevance to better understand and apply improvement technologies in agriculture.

Limitations of the study

In this study, we have illustrated that TOR by sensing spermidine sufficiency can regulate spermidine homeostasis by promoting translation reinitiation of uORF-containing mRNAs encoding polyamine degrading enzymes. Although we have analyzed expression levels of enzymes involved in polyamine catabolism in plants, further systematic analysis of mRNA translation efficiencies encoding both the polyamine biosynthesis and degradation enzymes in different TOR contrasting conditions is necessary to understand the fundamental principles of this regulation. Combining our approach with the direct analysis of endogenous levels of spermidine and other polyamines, that is beyond the scope of this study, will enhance our understanding of how polyamine homeostasis is regulated by TOR. In addition, the molecular analysis could be extended to different developmental stages.

STAR★METHODS

Detailed methods are provided in the online version of this paper and include the following:

- KEY RESOURCES TABLE
- RESOURCE AVAILABILITY
  - Lead contact
  - Materials availability
  - Data and code availability
- EXPERIMENTAL MODEL AND SUBJECT DETAILS
- METHOD DETAILS
  - Maize growth conditions and treatments
  - *Arabidopsis* seedlings growth conditions
  - Seedling phenotyping

- Protein extraction
- Western blot analysis
- Polyribosome fractionation
- RNA analysis
- Construct generation for protoplast transfections
- *Arabidopsis* protoplast preparation and GUS activity measurement

● QUANTIFICATION AND STATISTICAL ANALYSIS

SUPPLEMENTAL INFORMATION

Supplemental information can be found online at https://doi.org/10.1016/j.isci.2021.103260.

ACKNOWLEDGMENTS

We thank A. von Arnim for providing crucial antibodies for these studies, R. A. Urquidi Camacho and A. von Arnim for providing an uORF database for Arabidopsis genes, and A. Geldreich for excellent technical support. We appreciate the use of core facilities at Unidad de Servicios de Apoyo a la Investigación y la Industria (USAII) and technical support from Jorge Herrera-Díaz.

This work was funded by UNAM-PAPIIT IN218921, IN214118 and Facultad de Química-UNAM PAIP 5000-9118 to TDD; a CONACyT PhD fellowship program to KSD; French Agence Nationale de la Recherche—ANR-18-CE13-0019 – "ReinitiaTOR" to LR, and 2020 Marie Curie fellowship 885864 "TOR in acTIon" MSCA-IF-EF-ST to YD.

AUTHOR CONTRIBUTIONS

Conceived and designed the project: YD, LR, KSD, and TDD. Performed the experiments: KSD, YD, CP, EMFR, and GOB. Analyzed the data: KSD, YD, CP, LR, and TDD. Designed the regulatory model: YD and LR. Wrote and revised the paper: YD, KSD, LR, and TDD. All authors approved the final version. KSD performed her Ph.D. studies in TDD lab and a 3-month internship in LR lab.

DECLARATION OF INTERESTS

The authors declare no competing interests.

Received: July 27, 2020
Revised: April 23, 2021
Accepted: October 11, 2021
Published: November 19, 2021

REFERENCES

Agredano-Moreno, L.T., Reyes de la Cruz, H., Martínez-Castilla, L.P., and Sánchez de Jiménez, E. (2007). Distinctive expression and functional regulation of the maize (Zea mays L.) TOR kinase ortholog. Mol. Biosyst. *3*, 794–802.

Anderson, G.H., Veit, B., and Hanson, M.R. (2005). The Arabidopsis AtRaptor genes are essential for post-embryonic plant growth. BMC Biol. *3*, 12.

von Arnim, A.G., Jia, Q., and Vaughn, J.N. (2014). Regulation of plant translation by upstream open reading frames. Plant Sci. *214*, 1–12.

Caldana, C., Li, Y., Leisse, A., Zhang, Y., Bartholomaeus, L., Fernie, A.R., Willmitzer, L., and Giavalisco, P. (2013). Systemic analysis of inducible target of rapamycin mutants reveal a general metabolic switch controlling growth in Arabidopsis thaliana. Plant J. *73*, 897–909.

Cao, P., Kim, S.J., Xing, A., Schenck, C.A., Liu, L., Jiang, N., Wang, J., Last, R.L., and Brandizzi, F. (2019). Homeostasis of branched-chain amino acids is critical for the activity of TOR signaling in Arabidopsis. Elife *8*, e50747.

Casagrande Figuereido, V., Markworth, J.F., and Cameron-Smith, D. (2017). Considerations on mTOR regulation at serine 2448: implications for muscle metabolism studies. Cell. Mol. Life Sci. *74*, 2537–2545.

Chen, D., Shao, Q., Yin, L., Younis, A., and Zheng, B. (2019). Polyamine function in plants: metabolism, regulation on development, and roles in abiotic stress responses. Front. Plant Sci. *9*, 1945.

Crombez, H., Roberts, I., Vangheluwe, N., Motte, H., Jansen, L., Beeckman, T., and Parizot, B. (2016). Lateral root inducible system in Arabidopsis and maize. J. Vis. Exp. *107*, e53481.

Deprost, D., Truong, H.N., Robaglia, C., and Meyer, C. (2005). An Arabidopsis homolog of RAPTOR/KOG1 is essential for early embryo development. Biochem. Biophys. Res. Commun. *326*, 844–850.

Deprost, D., Yao, L., Sormani, R., Moreau, M., Leterreux, G., Nicolaï, M., Bedu, M., Robaglia, C., and Meyer, C. (2007). The Arabidopsis TOR kinase links plant growth, yield, stress resistance and mRNA translation. EMBO Rep. *8*, 864–870.

Díaz-Granados, V.H., López-López, J.M., Flores-Sánchez, J., Olguin-Alor, R., Bedoya-López, A., Dinkova, T.D., Salazar-Díaz, K., Vázquez-Santana, S., Vázquez-Ramos, J.M., and Lara-Núñez, A. (2020). Glucose modulates proliferation in root apical meristems via TOR in maize during germination. Plant Physiol. Biochem. *155*, 126–135.

Dinkova, T.D., de la Cruz, H.R., García-Flores, C., Aguilar, R., Jiménez-García, L.F., and de Jiménez, E.S. (2007). Dissecting the TOR–S6K signal transduction pathway in maize seedlings: relevance on cell growth regulation. Physiol. Plant *130*, 1–10.

Dobrenel, T., Mancera-Martínez, E., Forzani, C., Azzopardi, M., Davanture, M., Moreau, M., Schepetilnikov, M., Chicher, J., Langella, O., Zivy, M., et al. (2016). The Arabidopsis TOR kinase specifically regulates the expression of nuclear genes coding for plastidic ribosomal proteins and the phosphorylation of the cytosolic ribosomal protein S6. Front. Plant Sci. *7*, 1611.

Dong, P., Xiong, F., Que, Y., Wang, K., Yu, L., Li, Z., and Ren, M. (2015). Expression profiling and functional analysis reveals that TOR is a key player in regulating photosynthesis and phytohormone signaling pathways in Arabidopsis. Front. Plant Sci. *6*, 677.

Dong, Y., Silbermann, M., Speiser, A., Forieri, I., Linster, E., Poschet, G., Allboje Samami, A., Wanatabe, M., Sticht, C., Teleman, A.A., et al. (2017). Sulfur availability regulates plant growth via glucose-TOR signaling. Nat. Commun. *8*, 1174.

Duan, J., Li, J., Guo, S., and Kang, Y. (2008). Exogenous spermidine affects polyamine metabolism in salinity-stressed Cucumis sativus roots and enhances short-term salinity tolerance. J. Plant Physiol. *165*, 1620–1635.

Enganti, R., Cho, S.K., Toperzer, J.D., Urquidi-Camacho, R.A., Cakir, O.S., Ray, A.P., Abraham, P.E., Hettich, R.L., and von Arnim, A.G. (2018). Phosphorylation of ribosomal protein RPS6 integrates light signals and circadian clock signals. Front. Plant Sci. *8*, 2210.

Franceschetti, M., Hanfrey, C., Scaramagli, S., Torrigiani, P., Bagni, N., Burtin, D., and Michael, A.J. (2001). Characterization of monocot and dicot plant S-adenosyl-l-methionine decarboxylase gene families including identification in the mRNA of a highly conserved pair of upstream overlapping open reading frames. Biochem. J. *353*, 403–409.

Garrocho-Villegas, V., Aguilar C, R., and Sánchez de Jiménez, E. (2013). Insights into the TOR-S6K signaling pathway in maize (Zea mays L.). Pathway activation by effector-receptor interaction. Biochemistry *52*, 9129–9140.

Gu, X., Orozco, J.M., Saxton, R.A., Condon, K.J., Liu, G.Y., Krawczyk, P.A., Scaria, S.M., Harper, J.W., Gygi, S.P., and Sabatini, D.M. (2017). SAMTOR is an S-adenosylmethionine sensor for the mTORC1 pathway. Science *358*, 813–818.

Guerrero-González, M.L., Ortega-Amaro, M.A., Juárez-Montiel, M., and Jiménez-Bremont, J.F. (2014). Arabidopsis Polyamine oxidase-2 uORF is required for downstream translational regulation. Plant Physiol. Biochem. *108*, 381–390.

Hanfrey, C., Elliott, K.A., Franceschetti, M., Mayer, M.J., Illingworth, C., and Michael, A.J. (2005). A dual upstream open reading frame-based autoregulatory circuit controlling polyamine-responsive translation. J. Biol. Chem. *280*, 39229–39237.

Hill, J.R., and Morris, D.R. (1992). Cell-specific translation of S-adenosylmethionine decarboxylase mRNA. Regulation by the 5′ transcript leader. J. Biol. Chem. *267*, 21886–21893.

Huang, Y., Lin, C., He, F., Li, Z., Guan, Y., Hu, Q., and Hu, J. (2017). Exogenous spermidine improves seed germination of sweet corn via involvement in phytohormone interactions, H2O2 and relevant gene expression. BMC Plant Biol. *17*, 1.

Hummel, I., Couée, I., El Amrani, A., Martin-Tanguy, J., and Hennion, F. (2002). Involvement of polyamines in root development at low temperature in the subantarctic cruciferous species *Pringlea antiscorbutica*. J. Exp. Bot. *53*, 1463–1473.

Imai, A., Akiyama, T., Kato, T., Sato, S., Tabata, S., Yamamoto, K.T., and Takahashi, T. (2004a). Spermine is not essential for survival of Arabidopsis. FEBS Lett. *556*, 148–152.

Imai, A., Matsuyama, T., Hanzawa, Y., Akiyama, T., Tamaoki, M., Saji, H., Shirano, Y., Kato, T., Hayashi, H., Shibata, D., et al. (2004b). Spermidine synthase genes are essential for survival of Arabidopsis. Plant Physiol. *135*, 1565–1573.

Jiménez-Bremont, J.F., Ruiz, O.A., and Rodríguez-Kessler, M. (2007). Modulation of spermidine and spermine levels in maize seedlings subjected to long-term salt stress. Plant Physiol. Biochem. *45*, 812–821.

Jing, J., Guo, S., Li, Y., and Li, W. (2020). The alleviating effect of exogenous polyamines on heat stress susceptibility of different heat resistant wheat (Triticum aestivum L.) varieties. Sci. Rep. *10*, 7467.

Kravchenko, A., Citerne, S., Jéhanno, I., Bersimbaev, R.I., Veit, B., Meyer, C., and Leprince, A.S. (2015). Mutations in the Arabidopsis Lst8 and Raptor genes encoding partners of the TOR complex, or inhibition of TOR activity decrease abscisic acid (ABA) synthesis. Biochem. Biophys. Res. Commun. *467*, 992–997.

Li, X., Cai, W., Liu, Y., Li, H., Fu, L., Liu, Z., Xu, L., Liu, H., Xu, T., and Xiong, Y. (2017). Differential TOR activation and cell proliferation in Arabidopsis root and shoot apexes. Proc. Natl. Acad. Sci. U S A *114*, 2765–2770.

Liko, D., and Hall, M., N. (2015). mTOR in health and in sickness. J. Mol. Medicine *93*, 1061–1073.

Liu, G.Y., and Sabatini, D.M. (2020). mTOR at the nexus of nutrition, growth, ageing and disease. Nat. Rev. Mol. Cell Biol. *21*, 183–203.

Mahfouz, M.M., Kim, S., Delauney, A.J., and Verma, D.P. (2006). Arabidopsis TARGET OF RAPAMYCIN interacts with RAPTOR, which regulates the activity of S6 kinase in response to osmotic stress signals. Plant Cell *18*, 477–490.

Majumdar, R., Shao, L., Turlapati, S.A., and Minocha, S.C. (2017). Polyamines in the life of Arabidopsis: profiling the expression of S-adenosylmethionine decarboxylase (SAMDC) gene family during its life cycle. BMC Plant Biol. *17*, 264.

Menand, B., Desnos, T., Nussaume, L., Berger, F., Bouchez, D., Meyer, C., and Robaglia, C. (2002). Expression and disruption of the Arabidopsis TOR (target of rapamycin) gene. Proc. Natl. Acad. Sci. U S A *99*, 6422–6427.

Montané, M.H., and Menand, B. (2013). ATP-competitive mTOR kinase inhibitors delay plant growth by triggering early differentiation of meristematic cells but no developmental patterning change. J. Exp. Bot. *64*, 4361–4374.

Moreau, M., Azzopardi, M., Clément, G., Dobrenel, T., Marchive, C., Renne, C., Martin-Magniette, M.L., Taconnat, L., Renou, J.P., Robaglia, C., et al. (2012). Mutations in the Arabidopsis homolog of LST8/GβL, a partner of the target of rapamycin kinase, impair plant growth, flowering, and metabolic adaptation to long days. Plant Cell *24*, 463–481.

Moschou, P.N., Wu, J., Cona, A., Tavladoraki, P., Angelini, R., and Roubelakis-Angelakis, A. (2012). The polyamines and their catabolic products are significant players in the turnover of nitrogenous molecules in plants. J. Exp. Bot. *63*, 5003–5015.

Mostofa, M.G., Yoshida, N., and Fujita, M. (2014). Spermidine pretreatment enhances heat tolerance in rice seedlings through modulating antioxidative and glyoxalase systems. Plant Growth Regul. *73*, 31–44.

Ren, M., Venglat, P., Qiu, S., Feng, L., Cao, Y., Wang, E., Xiang, D., Wang, J., Alexander, D., Chalivendra, S., et al. (2012). Target of rapamycin signaling regulates metabolism, growth, and life span in Arabidopsis. Plant Cell *24*, 4850–4874.

Rodríguez, A.A., Maiale, S.J., Menéndez, A.B., and Ruiz, O.A. (2009). Polyamine oxidase activity contributes to sustain maize leaf elongation under saline stress. J. Exp. Bot. *60*, 4249–4262.

Ryabova, L.A., and Hohn, T. (2000). Ribosome shunting in the cauliflower mosaic virus 35S RNA leader is a special case of reinitiation of translation functioning in plant and animal systems. Genes Dev. *14*, 817–829.

Ryabova, L.A., Robaglia, C., and Meyer, C. (2019). Target of Rapamycin kinase: central regulatory hub for plant growth and metabolism. J. Exp. Bot. *70*, 2211–2216.

Saxton, R.A., and Sabatini, D.M. (2017). mTOR signaling in growth, metabolism, and disease. Cell *168*, 960–976.

Schepetilnikov, M., and Ryabova, L.A. (2017). Auxin signaling in regulation of plant translation reinitiation. Front. Plant Sci. *8*, 1014.

Schepetilnikov, M., Kobayashi, K., Geldreich, A., Caranta, C., Robaglia, C., Keller, M., and Ryabova, L.A. (2011). Viral factor TAV recruits TOR/S6K1 signalling to activate reinitiation after long ORF translation. EMBO J. *30*, 1343–1356.

Schalm, S.S., and Blenis, J. (2002). Identification of a conserved motif required for mTOR signaling. Curr. Biol. *12*, 632–639.

Schepetilnikov, M., Dimitrova, M., Mancera-Martínez, E., Geldreich, A., Keller, M., and Ryabova, L.A. (2013). TOR and S6K1 promote translation reinitiation of uORF-containing mRNAs via phosphorylation of eIF3h. EMBO J. *32*, 1087–1102.

Schepetilnikov, M., Makarian, J., Srour, O., Geldreich, A., Yang, Z., Chicher, J., Hammann, P., and Ryabova, L.A. (2017). GTPase ROP2 binds and promotes activation of target of rapamycin, TOR, in response to auxin. EMBO J. *36*, 886–903.

Shantz, L.M., Viswanath, R., and Pegg, A.E. (1994). Role of the 5′-untranslated region of mRNA in the

synthesis of S-adenosylmethionine decarboxylase and its regulation by spermine. Biochem. J. *302*, 765–772.

Shi, L., Wu, Y., and Sheen, J. (2018). TOR signaling in plants: conservation and innovation. Development *145*, dev160887.

Tang, S., Zhang, H., Li, L., Liu, X., Chen, L., Chen, W., and Ding, Y. (2018). Exogenous spermidine enhances the photosynthetic and antioxidant capacity of rice under heat stress during early grain-filling period. Funct. Plant Biol. *45*, 911–921.

Tiburcio, A.F., Altabella, T., Bitrián, M., and Alcázar, R. (2014). The roles of polyamines during the lifespan of plants: from development to stress. Planta *240*, 1–18.

Turck, F., Zilbermann, F., Kozma, S.C., Thomas, G., and Nagy, F. (2004). Phytohormones participate in an S6 kinase signal transduction pathway in Arabidopsis. Plant Physiol. *134*, 1527–1535.

Untergasser, A., Nijveen, H., Rao, X., Bisseling, T., Geurts, R., and Leunissen, J.A. (2007). Primer3Plus, an enhanced web interface to Primer3. Nucleic Acids Res. *35*, W71–W74.

Woodhouse, M.R., Cannon, E.K., Portwood, J.L., Harper, L.C., Gardiner, J.M., Schaeffer, M.L., and Andorf, C.M. (2021). A pan-genomic approach to genome databases using maize as a model system. BMC Plant Biol. *21*, 385.

Xiong, Y., and Sheen, J. (2012). Rapamycin and glucose-target of rapamycin (TOR) protein signaling in plants. J. Biol. Chem. *287*, 2836–2842.

Xiong, Y., McCormack, M., Li, L., Hall, Q., Xiang, C., and Sheen, J. (2013). Glucose-TOR signalling reprograms the transcriptome and activates meristems. Nature *496*, 181–186.

Yoo, S.D., Cho, Y.H., and Sheen, J. (2007). Arabidopsis mesophyll protoplasts: a versatile cell system for transient gene expression analysis. Nat. Protoc. *2*, 1565–1572.

Zabala-Letona, A., Arruabarrena-Aristorena, A., Martín-Martín, N., Fernandez-Ruiz, S., Sutherland, J.D., Clasquin, M., Tomas-Cortazar, J., Jimenez, J., Torres, I., Quang, P., et al. (2017). mTORC1-dependent AMD1 regulation sustains polyamine metabolism in prostate cancer. Nature *547*, 109–113.

STAR★METHODS

KEY RESOURCES TABLE

REAGENT or RESOURCE	SOURCE	IDENTIFIER
Antibodies		
AtrpS6	Enganti et al. (2018)	N/A
AtrpS6-P(S240)	Enganti et al. (2018)	N/A
AtS6K1/2	Agrisera	Cat#AS121855; RRID: AB_2832919
Goat anti-rabbit IgG:HRP	Southern Biotech	Cat#4030-05; RRID: AB_2687483
mTOR-P(S2448)	Santa Cruz Biotech	Cat# c-293133; RRID: AB_2861149
S6K1-P(T449)	Abcam	Cat# ab207399
Chemicals, peptides, and recombinant proteins		
1-Naphtalen Acetic Acid (1-NAA)	Sigma-Aldrich	Cat#N0640
AZD-8055	Chemdea	Cat#CD0348
Complete ^{TM}, EDTA-free Protease Inhibitor Cocktail	Roche Molecular Diagnostics	Cat#04693132001
Cycloheximide	Sigma-Aldrich	Cat#01810
Cyclohexylamine (CHA)	Sigma-Aldrich	Cat#240648
Halt-Phosphatase Inhibitor Cocktail 100X	Thermo Scientific	Cat#78420
Heparin	Sigma-Aldrich	Cat#H3149
MES	Sigma-Aldrich	Cat#M3671
Murashige and Skoog (MS) medium	Sigma-Aldrich	Cat#M5519
Proteinase K	Sigma-Aldrich	Cat#P2308
Spermidine (Spd)	Sigma-Aldrich	Cat#S2626
Critical commercial assays		
Improm-II Reverse Transcriptase	Promega	Cat#A3800
Luminata Classic Western HRP Substrate	Merck Millipore	Cat#WBLUC0500
Maxima SYBR Green/ROX qPCR Master Mix	Thermo Scientific	Cat#K0221
4-MUG for GUS detection	Sigma-Aldrich	Cat#M9130
Trizol reagent	Thermo Scientific	Cat#15596026
RNA Clean and Concentrator	Zymo Research	Cat#R1013
Experimental models: Organisms/strains		
Arabidopsis thaliana Columbia ecotype Col-0	ABRC	CS22625
Arabidopsis *tor* RNAi line 35-7	Deprost et al. (2007)	N/A
Arabidopsis *s6k1-1* mutant line	ABRC	Salk_148694
Arabidopsis thaliana *raptor* mutant line *rap78*	Deprost et al. (2005)	Salk_078159
Oligonucleotides		
Primers for maize transcripts, see Table S1	This paper	N/A
Recombinant DNA		
pAtCuAO1 5'UTR-GUS	This study	N/A
pmonoGFP	(Schepetilnikov et al., 2013)	N/A
pmonoGUS	(Schepetilnikov et al., 2013)	N/A
pZmPAO3 5'UTR-GUS	This study	N/A
Software and algorithms		
ImageJ	N/A	https://imagej.net
Excel	Microsoft	N/A

(*Continued on next page*)

Continued

REAGENT or RESOURCE	SOURCE	IDENTIFIER
Gene Infinity – ORF Finder	N/A	http://www.geneinfinity.org/sms/sms_orffinder.html
BoxPlotR	N/A	http://shiny.chemgrid.org/boxplotr/
Primer3 Plus	Untergasser et al. (2007)	http://primer3plus.com/cgi-bin/dev/primer3plus.cgi
Deposited Data		
Arabidopsis transcriptome for *tor* RNAi plants	Caldana et al. (2013)	GSE38878
Arabidopsis transcriptome in response to Glucose	Xiong et al. (2013)	GSE40245

RESOURCE AVAILABILITY

Lead contact

- Further information and requests for resources and reagents should be directed to and will be fulfilled by the lead contact, Lyubov A. Ryabova (lyuba.ryabova@ibmp-cnrs.unistra.fr)

Materials availability

- Plasmids and seeds used in this study are available with a completed Materials Transfer Agreement Request for these materials by submitting to Dr. L.A. Ryabova (lyuba.ryabova@ibmp-cnrs.unistra.fr).

Data and code availability

- This paper analyzes existing, publicly available data. The accession numbers for analyzed datasets are listed in the key resources table.
- This paper does not report original code.
- Any additional information required to reanalyze the data reported in this paper is available from the lead contact upon request.

EXPERIMENTAL MODEL AND SUBJECT DETAILS

Mexican maize (*Zea mays* L. cv. Chalqueño) seeds (Spring 2018) were used dry or between one and six days upon imbibition. For *Arabidopsis thaliana*, the ecotype Columbia-0, *tor* RNAi line 35-7 (Deprost et al., 2007), *s6k1-1* mutant (Salk_148694) and Raptor mutant *rap78* (Salk_078159) were used at 14 days upon imbibition.

METHOD DETAILS

Maize growth conditions and treatments

For germination experiments Mexican maize (*Zea mays* L. cv. Chalqueño) seeds (Spring 2018) were imbibed on moisturized cotton at 26 ($\pm$2°C) in the darkness for 24 or 48 h. Short treatments with the TOR inhibitor AZD-8055 were performed during the last three hours of imbibition of 48 h excised axes to evaluate TOR pathway activity and polysomal profiles. To test the concentration-dependent inhibitor effect, embryonic axes dissected from 24 h imbibed seeds were placed on a cotton moisturized with 1/2 Murashige and Skoog (MS) $\pm$ AZD-8055 (5 μM, 10 μM, 20 μM) during additional 72 h at 28°C in the darkness.

For long-term seedling growth phenotyping and treatments, whole seeds were rolled in a paper towel and placed vertically in a cylindrical container under 16 h light/8 h darkness photoperiod at 28°C as described previously (Crombez et al., 2016). The paper towel was imbibed in water (mock), 50 μM AZD-8055 (AZD), 0.1 mM (for non-germinated seeds) or 0.2 mM (for germinated seeds) Spermidine (Spd), or combination of both (Spd/AZD).

Higher concentration of AZD-8055 was employed for whole seed incubations due to the starchy endosperm seed barrier as reported for cereals, including maize (Montané and Menand, 2013; Díaz-Granados et al., 2020). For cyclohexylamine (CHA) treatments, 24 h imbibed seeds were treated with 1 mM CHA alone or with 0.2 mM Spd and phenotype was registered after 48 h of the treatment. AZD-8055 was dissolved in Dimethyl Sulphoxide (DMSO) and CHA in water. Equivalent amount of DMSO was added to mock for AZD inhibition experiments.

Since cyclohexylamine (CHA) is a competitive inhibitor of Spd synthase (SPDS), which competes with Put for SPDS binding, we used 1 mM CHA to ensure competition with Put and evaluate the effect of exogenous Spd used at 0.1 mM concentration. 2 mM CHA was used for dicot plants in Hummel et al. (2002).

For heat stress, germinated seeds were grown at 28°C for 72 hours under the indicated treatments, after which those were separated in two groups. One group was maintained at 28°C, whereas the other was transferred to a chamber at 42°C, for additional 72 h under the same treatments.

Arabidopsis seedlings growth conditions

Arabidopsis thaliana ecotype Columbia-0 seeds were used for all experiments. The *tor* RNAi line 35-7 was previously described (Deprost et al., 2007). Raptor mutant *rap78* (Salk_078159) was provided by C. Meyer (INRA, Versailles, France). *Arabidopsis* seeds were cultured on squared plates containing 1/2 MS, 0.5% sucrose and 0.8% agar medium for two weeks under 16 h light/ 8 h darkness photoperiod at 21°C. Treatments of 0.2 μM AZD-8055 (AZD), 0.01 mM or 0.1 mM Spermidine (Spd) and double treatment for each Spd concentration (AZD/Spd) were included in the medium. To analyse the growth phenotype caused by AZD, Spd or combination, we used lower AZD concentration than previously reported (Schepetilnikov et al., 2017) to avoid causing dramatic growth phenotype (Montané and Menand, 2013) and allowing to study sensitivity to Spd.

Seedling phenotyping

After each imbibition time and treatment, maize seeds were photographed and length measurements of whole embryonic axe, the principal root or the shoot were performed using the Image J software. For *Arabidopsis thaliana*, root measurements corresponded to the end of the experiment (two weeks).

Protein extraction

Total proteins were extracted from half gram of maize whole embryonic axes or root tips (1.0 cm from the tip) to evaluate activation of TOR-S6K during germination and seedling establishment. To analyze the effect of different AZD-8055 concentrations, protein extractions were made from whole embryonic axes. To analyze effects of Spd, CHA or both Spd and CHA treatment on TOR signaling pathway activation, treatments were performed for 24 hours on excised embryonic axes from 24 h imbibed seeds.

Maize tissues were homogenized in extraction buffer [50 mM HEPES pH 7.6, 4 mM EDTA, 20 mM EGTA, 20 mM mannitol, 0.2 mM PMSF, 1X Halt Phosphatase Inhibitor Cocktail (ThermoFischer), and Protease Inhibitor CompleteTM (Roche Diagnostics)], cleared by centrifugation for 40 min, and determined for protein concentration by Bradford. Protein extractions for *Arabidopsis* were performed from whole seedlings at the end of treatments using 2X Laemmli buffer. About 10-20 μg of total protein from *Arabidopsis*, 100 μg (TOR-P) and 40 μg (S6K, S6K-P, rpS6, rpS6-P) of total protein extract from maize were loaded per line.

Western blot analysis

Protein extracts were separated by 7% (TOR) or 12% (S6K and rpS6) SDS-PAGE and electroblotted onto polyvinylidene fluoride (PVDF) membrane. The membrane was blocked with 5 % (w/v) fat-free milk in 1X PBS, pH 7.4 and incubated overnight at 4°C (primary polyclonal antibodies) or during 3 h (monoclonal antibodies) at the appropriate dilutions prepared in 1X PBS/0.1% (v/v) Tween-20. The following primary antibodies were used in this study: AtrpS6 (Enganti et al., 2018, 1:2500), AtrpS6-P(S240) (Enganti et al., 2018, 1:5000), AtS6K1/2 (Agrisera, AS121855, 1:5000), mTOR-P(S2448) (Santa Cruz Biotech, SC-293133, 1:200), S6K1-P(T449) (Abcam, ab207399, 1:5000). The secondary antiserum (Goat anti-rabbit IgG:HRP, Bio-Rad, 403005) was used at 1:5,000 dilution and incubated for 2 h at room temperature. Blots were developed with Luminata Classic Western HRP Substrate from Millipore. All antibodies had been previously used in *Arabidopsis* (Schepetilnikov et al., 2013; Cao et al., 2019) and maize (Garrocho-Villegas et al., 2013; Díaz-Granados et al., 2020) reports. Full size Western blots with molecular weight indications are shown for each antibody/species in supplemental information file (Data S1). Migration of the endogenous unphosphorylated S6K is unusual, since it shows retardation on the gel (around 65 kDa), possibly due to particularities of the plant protein, such acidic residues or unstructured N- and C-terminal regions interfering with SDS interaction. However, upon urea application, S6K1 migrates on SDS-PAGE at about 53 kDa as shown in

Data S1. Further, the 65 kDa band detected by anti-AtS6K1/2 (Agrisera) appears reduced in a *s6k1-1* mutant (Salk_148694), as does the 53 kDa band detected by anti-S6K1-P (Abcam).

Polyribosome fractionation

One gram of whole embryonic axes was ground with liquid nitrogen in a mortar and homogenized in 5 ml of lysis buffer consisting of 200 mM Tris-HCl pH 8.5, 50 mM KCl, 25 mM $MgCl_2$, 2 mM EGTA, 2% PTE (10 Tridecyl Polyoxyethylene ether), 1% IGEPAL, 1% Triton X-100, 0.1% DTT 1 M, 0.2 mg/mL cycloheximide and 0.5 mg/mL Heparin. The slurry was cleared twice from debris at 12,000 x g for 15 min, 4°C and the supernatant was applied onto 2 ml of 60% sucrose cushion in gradient buffer (50 mM Tris-HCl pH 8.5, 20 mM KCl, 10 mM $MgCl_2$) to enrich ribosomes by 3 h-centrifugation at 50,000 rpm, 4°C in a fixed angle rotor 80Ti. The precipitate was dissolved in 300-400 µl extraction buffer, applied to a continuous 15% to 60% sucrose density gradient and centrifuged at 38,000 rpm, 4°C for 2 h in a swinging rotor SW 55Ti. Gradients were collected in 500 µl fractions with a Labconco bomb connected to Econo UV Monitor (BioRad) for continuous absorbance monitoring at 260 nm. According to the 260 nm profiles, fractions were pooled as NR (no ribosome), 80S (monosomes), LP (low polysomes), MP (medium polysomes) and HP (high polysomes).

RNA analysis

Total RNA was extracted using TRIzol Reagent. RNA from polysomal profiling was obtained by pooled fractions treatment with 25 µl of 10% sodium dodecyl sulfate (SDS) and 1 µl of 10 mg/ml proteinase K for 30 min at 37°C, extraction with 250 µl of acid phenol and 250 µl of chloroform: iso-amyl alcohol (24:1) and precipitation with 70 µl of 10 M LiCl and 470 µl isopropanol. Precipitated RNA was washed with 70 % ethanol, briefly air-dried and dissolved in 30 µl of DEPC-treated water. Total and polysomal RNAs were subjected to DNase treatment and purification by RNA Clean and Concentrator kit, followed by reverse transcription with Improm-II Reverse Transcriptase and either end- point PCR (polysomal fractions) or real-time PCR (total RNA) using Maxima SYBR Green/ROX qPCR Master Mix. Gene-specific primers were designed with Primer3 Plus (Untergasser et al., 2007) and are available in Table S1. Relative expression levels were computed by $2^{-\Delta\Delta CT}$ method using actin as housekeeping control in two independent biological replicate experiments.

Construct generation for protoplast transfections

Standard short UTR p*monoGUS* and p*monoGFP* were used as basal translation and transfection controls, respectively (Schepetilnikov et al., 2011, 2013). The p*AtCuAO1-GUS* and p*ZmPAO3-GUS* constructs [*AtCuAO1 5'UTR-GUS*; *ZmPAO3 5'UTR-GUS*] were generated by substitution of a short *CAMV* sequence in p*mono*GUS plasmid with the *AtCuAO1* (At1g62810) 5'UTR or *ZmPAO3* (Zm00001d001883) 5'UTR, downstream of the constitutive 35S promoter and upstream of the start codon of the *GUS* reporter. Primers used for 5'UTR amplification were: *CuAO1-UTR*-FW: acgcgtcgacGCGTTTGTAATGACATGAACATG; *CuAO1-UTR*-RV: gggtttctacaggacgtaaCATCGATTGAGTGAGAGTTTTTG *ZmPAO3-UTR*-FW: ggggtacccACCCG TGTCGTGTCTAAACGGAC; *ZmPAO3-UTR*-RV: ggggtacccccggtataccgACCAGCCGCCGGCTTCG. Small case letters indicate added nucleotides including sites for restriction enzymes KpnI and AccI (underlined) used to clone the 5'UTR within p*monoGUS*. The construct *pAtARF3-GUS* was described in Schepetilnikov et al. (2013).

Arabidopsis protoplast preparation and GUS activity measurement

Transient expression of constructs and GUS activity assays in *Arabidopsis* mesophyll protoplasts were conducted according to (Schepetilnikov et al., 2013; Yoo et al., 2007) with minimal modifications. Five micrograms p*AtCuAO1-GUS*, or 5 µg p*ZmPAO3-GUS*, or 10 µg p*AtARF3-GUS* or 5 µg p*monoGUS* were used for co-transformation of *Arabidopsis* mesophyll protoplasts with 5 µg p*monoGFP* as transfection control (see Figure 3D). Transfected protoplasts were incubated in WI buffer including 1 µM auxin (1-NAA), or 0.1 mM Spd with or without 0.5 µM AZD-8055 overnight at 26°C in WI buffer (4 mM MES pH 5.7, 0.5 M mannitol, 20 mM KCl) under darkness. After overnight incubation transfected protoplasts were harvested by centrifugation and resuspended in GUS extraction buffer (50 mM NaH_2PO_4 pH 7.0, 10 mM EDTA, 0.1% NP-40). The aliquots were immediately taken for GUS reporter gene assays. GUS activity was measured by a fluorimetric assay using a FLUOstar OPTIMA fluorimeter (BMG Biotech) and normalized with respect to GUS RNA levels. The values given are the means from at least three independent experiments.

To estimate GUS RNA levels, total RNA from protoplasts was extracted using TRIzol. RNA samples were reverse transcribed into cDNA using SuperScript III reverse transcriptase with oligo-$(dT)_{18}$. sqRT-PCR

was performed with the pair of specific primers to the full-length *GUS* reporter gene. The PCR conditions were as follows: 2 min, 98°C (first cycle); 30 s, 98°C; 30 s, 56°C; 3 min, 72°C (20 cycles). PCR products were separated on a 1.2% agarose gel and visualized by ethidium bromide staining.

QUANTIFICATION AND STATISTICAL ANALYSIS

At least 15 seeds were used for each treatment in three independent biological experiments (n = 3). For seedling phenotyping and reporter construct expression in protoplasts under different treatments, statistical analysis was performed by One-way ANOVA followed by two-tailed t-test. For RT-qPCR experiments, statistical differences were evaluated by two-sample t-test. Asterisks indicate values that are significantly different from the relevant control *$p \leq 0.05$ **$p \leq 0.01$ ***$p \leq 0.001$ ****$p \leq 0.0001$. Graphs were generated with BoxPlotR. The statistical details of each experiment can be found in the corresponding figure legend.